Progress In Electromagnetics Research M, Vol. 46, 11–18, 2016

Simple Approach to Miniaturized Antenna Gain Measurement Using a Parallel Plate Cell in the HF Band

Evgueni Kaverine[1, *], Sebastien Palud[2], Franck Colombel[1], and Mohamed Himdi[1]

Abstract—This paper describes a method of measurement of miniaturized antenna gain in the HF band based on a parallel plate cell. Compared to a free space outdoor approach this method offers two advantages: the use of a well-defined environment and time efficiency. For the same external dimensions, it also has an advantage compared to TEM/GTEM cells designs in terms of the useful antenna under test (AUT) space. This space is of a major importance in the HF band since even miniature antennas can have considerable proportions. The proposed structure is composed of a parallel plate cell, whose construction is simple and not expensive. It offers a precision measurement with an error not exceeding 2.3 dB with respect to calibrated antenna gain and simulation results.

1. INTRODUCTION

The measurement of antenna gain in the HF band and below is a well-known challenge. Traditional methods, such as anechoic chambers, available from the UHF band and above, do not exist in the HF range due to low efficiency of absorbers and an important level of reflections occasioned by the walls of the chamber [1]. Outdoor free-space measurements also suffer from the considerable wavelength. Consequently, plane wave conditions (Eqs. (1)–(3)), defined in [2], are not easy to obtain and entail a huge distance between two antennas which compose the link budget. In addition, an interaction with the environment, a ground influence and reflections can compromise the accuracy of a gain measurement.

$$r_{ff} > \frac{2D^2}{\lambda} \tag{1}$$

$$r_{ff} \gg D \tag{2}$$

$$r_{ff} \gg \lambda \tag{3}$$

where r_{ff} is the far-field zone distance, D the largest dimension of the transmission antenna, and λ the wavelength.

Instead of trying to obtain a plane wave from a transmitting antenna, it can be easily created in a transmission line. The most famous example of such a line, called TEM cell, was proposed by Crawford in 1974 [3] with the main interest being electromagnetic compatibility: emission and susceptibility measurements, where the cell is acting as an E-field generator or a wide-band antenna, respectively. It is also used to calibrate E-field probes [4, 5] since the field strength is well defined, but also to expose biological samples [6], in order to evaluate the SAR (Specific Absorption Rate) or more generally an exposition level from the temperature rise. Finally, a TEM cell can be used to measure the gain of electrically small antennas. For the latter purpose, GTEM cells, which are high-frequency versions of TEM cells, are principally used as a less expensive alternative to anechoic chambers in the UHF band and above [7–12]. The main advantage of TEM/GTEM cells is their fully shielded structure preventing

Received 21 October 2015, Accepted 23 December 2015, Scheduled 13 January 2016

* Corresponding author: Evgueni Kaverine (evgueni.kaverine@univ-rennes1.fr).

[1] Institute of Electronics and Telecommunications of Rennes, UMR CNRS 6164, University of Rennes 1, France. [2] TDF Antenna Measurement Center, Liffré, France.

any radiation outside of the cell which can affect EMC/EMI measurements. However, the use of a septum highly reduces the useful space for the device under test which should not exceed a third of the height between the septum and the external shield. Such a small space generally limits the use of these cells to a component or board level.

This paper presents an alternative structure allowing the determination of the antenna gain in the HF band. It is based on a parallel plate cell, ancestor of TEM cell, and has an important advantage to provide a much larger useful space for the antenna under test (AUT) that, even miniaturized, can easily measure 60 cm. Other advantages of this structure are its simplicity, low-cost fabrication and lightweight. As TEM cells, a parallel plate cell (further PPC or cell) does not alter the characteristics (radiation pattern, input impedance etc.) of small antennas and accurately provides a plane wave distribution from DC to 30 MHz [13]. Because such a line is opened, it radiates some amount of injected energy. Whereas this unwanted radiation is of a big importance in EMC/EMI tests where a high magnitude field may be required. In the antenna gain measurement technique presented here, a field of some mV/m of magnitude is sufficient. In addition to such a weak E-field inside of a cell, an attenuation of 16.8 dB at 0.5 m from the PPC has been measured. All above means that the radiation outside of a cell is weak and does not interact a lot with the nearby environment. For the same reason, a normally shielded environment required by EMC/EMI measurements can be omitted [14].

The document is organized as follows. In Section 2, the measurement theory is briefly presented as well as the geometry of the PPC, field characteristics and measurement setup. In Section 3, we present results of some antenna gain measurements compared to simulated or certified gains.

2. DESIGN OF THE PPC

It is known that an EM plane wave produces a voltage drop across the antenna port depending on a co-polarized component of the E-field. This voltage is also directly related to the effective height of the antenna. In practice, the inverse of the effective height H_{eff}, called antenna factor (AF), is often used to describe the gain of an aerial.

$$AF = \frac{1}{H_{eff}} = \frac{E}{V_{port}} \tag{4}$$

where V_{port} is the voltage between the terminals of the antenna and E the amplitude of the E-field. In a 50 Ω system, the relation between the AF and the gain is:

$$G = \left(\frac{9.73}{\lambda\, AF}\right)^2 \tag{5}$$

In this way, the aim of the PPC is to provide stable and homogeneous field distribution of known magnitude which imitates the plane wave of a far-field zone.

The presented cell is a modified version of a cell which serves for EMI measurements respecting DIN 45305. The cell is presented in Figure 1. It is composed of two parallel aluminum plates which are 4 mm thick. Initially, the bottom of the cell was wider than the top, which caused an imbalance in the vertical distribution of the field between the plates. For that reason, the top plate was extended to the same size of 900 mm. However, we notice that the junctions between the parallel plates and tapered parts have discontinuities in width transition which may create some impedance mismatch and field perturbation, but these are not critical in the HF band considering the good accuracy of obtained results.

Since the only used propagation mode in any TEM type cell is the TEM mode, it is important to ensure that the cell is used below a certain cut-off frequency where a parasitic mode appears. The cut-off frequency of the first higher propagation mode, which is TE_{10}, of the PPC depends on the cell width (W) which is equal to some critical half wavelength $\lambda_{c(10)}/2$:

$$W = \frac{\lambda_{c(10)}}{2} \tag{6}$$

$$W = \frac{c}{2f_{c(10)}} \tag{7}$$

$$f_{c(10)} = \frac{c}{2W} \tag{8}$$

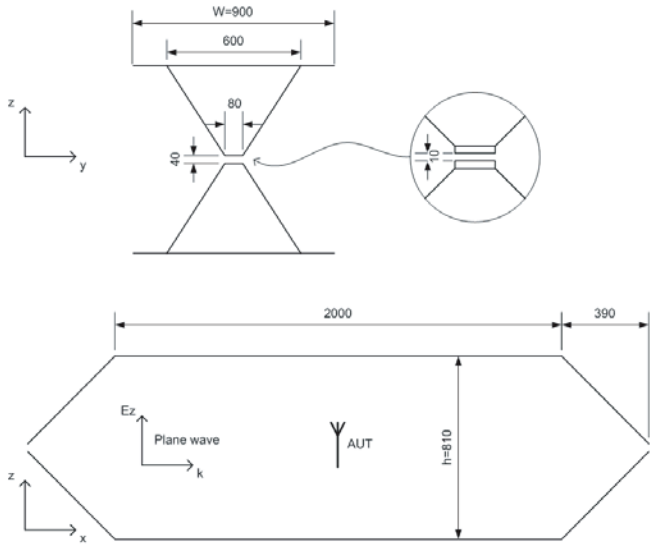

Figure 1. Geometry of the PPC after modification in YZ plane (top view) and XZ plane (bottom view). Dimensions in mm.

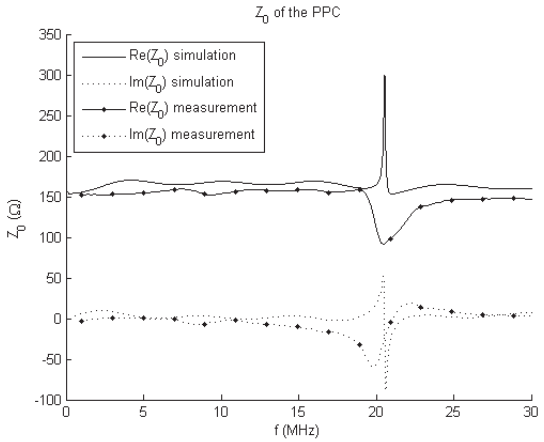

Figure 2. Characteristic impedance of the PPC.

where c is the speed of light in vacuum $\approx 3 \times 10^8$ m/s and W the width of the PPC shown in Figure 1.

Considering this width, the cut-off frequency $f_{c(10)}$ is situated at about 167 MHz which is high above the HF band of interest.

It was also important to verify the characteristic impedance Z_0 of the PPC. For this purpose, transmission line formula was used (Eq. (9)) where $Z_{s.c.}$ and $Z_{o.c.}$ are open and short-circuited impedances of the cell.

$$Z_0 = \sqrt{Z_{s.c.} Z_{o.c.}} \tag{9}$$

Resulting Z_0 shows (Figure 2) that the impedance of the cell is almost purely real and close to 150 Ω. Peak values spotted around 20 MHz can be neglected; this artifact is due to the electrical size of the cell equal to $\lambda/4$ at this frequency so that $Z_{s.c.}$ is transformed to $Z_{o.c.}$ and vise versa. In practice, the cell is loaded; therefore Z_0 remains constant.

Concerning the measurement setup (Figure 3), it is composed of a PPC loaded by a wide band 150 Ω precision (0.3%) resistor, a vector signal generator R&S SMIQ03B delivering continuous wave with an adjustable power and a receiver R&S ESH3 which measures the voltage drop at the antenna port in dBμV. Field strength is measured with a Narda NBM-550 field meter.

To maximize the delivered power to the cell and to prevent the creation of standing waves between the plates of the cell, an impedance transformer based on MCL T3-1T was used. Its aim is to transform the 50 Ω impedance of the signal generator into the 150 Ω characteristic impedance of the cell but also to balance currents on both plates. Consequently, the reflection coefficient of the cell is better than −20 dB (Figure 4).

Besides impedance matching, it was noted that the vertical E-field distribution is better when the cell is located at some height above a highly conductive ground. As mentioned above, even if shielded environment is not critical, the cell was put into an anechoic chamber 2 m above its metallic floor, in order to prevent any parasitic interference from the outdoor environment.

Since the measurement procedure needs an accurate knowledge of the E-field magnitude at any injected power, the first verification concerned the linearity of the response of the whole system (Figure 5). In this way, only one measurement of the field can be performed, then scaled to any input power. Due to the sensitivity of the Narda field meter, a power of +10 dBm was chosen.

Normally, Narda NBM-550 field meter provides a three-axial measurement in order to obtain a magnitude of each component of an E-field. However, since the cell is used in principal propagation TEM mode and considering the geometry and the orientation of the cell, the Ez component of the

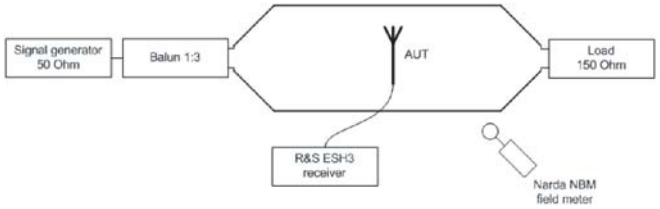

Figure 3. Measurement setup.

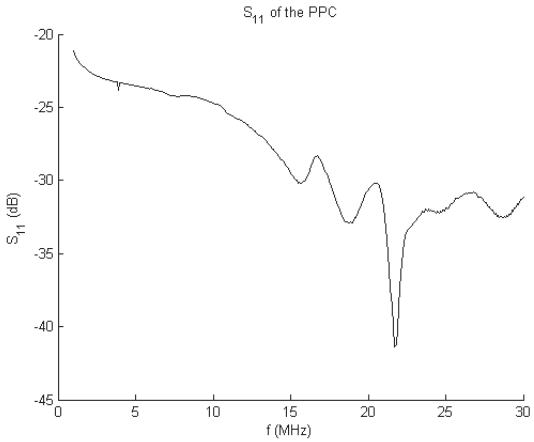

Figure 4. Measured S_{11} response of the loaded PPC with the balun.

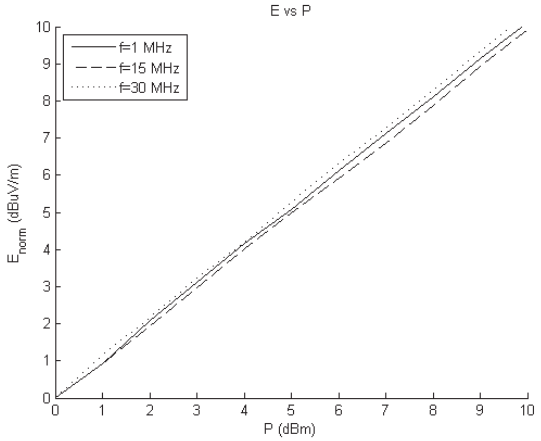

Figure 5. Measurement of the linearity of the system.

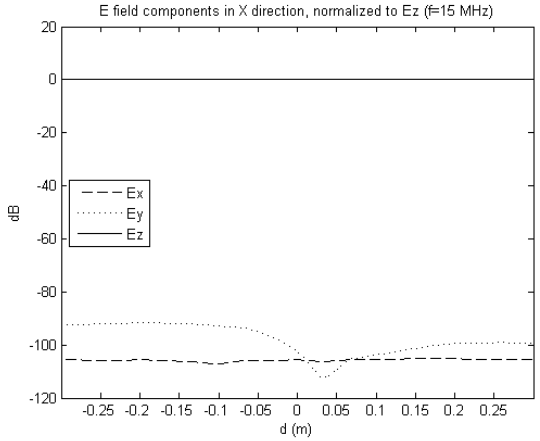

Figure 6. Simulated cross components of the E-field compared to Ez.

electric field largely dominates in the volume of interest (Figure 6). That is why either three axial measurement field meters or field meters giving only the average magnitude of the E-field can be used.

With the injected power of +10 dBm, the E-field strength varies from 122 to 124 dBμV/m depending on the frequency and the position of the field meter. For practical reasons, a volume equal to $0.6 \times 0.6 \times 0.6\,\mathrm{m}^3$ around the center of the cell, where the AUT can be put, has been studied in terms of field homogeneity. Simulated E-field distribution has almost constant magnitude in that region (Figures 7, 8). Measured field deviation in this volume does not exceed 0.6 dB compared to the field at the center of the PPC (Figure 9).

The field strength measured in five points along each axis is identical to CST Microwave Studio simulation result within a range of 1.5 dB (Table 1).

3. VALIDATION

3.1. Compared to Certified Antenna

To validate the measurement principle, a reference active loop antenna Lindgren 6502, having a certified antenna factor with a $+/-2$ dB tolerance, from 9 kHz to 30 MHz, was used. First of all, the field at the center of the PPC where the loop was put is measured using the Narda NBM-550 with an EF 0691 field

Table 1. Measurement/simulation difference of E-field along X, Y and Z directions (dB).

	d (m), X direction				
f (MHz)	−0.3	−0.15	0	0.15	0.3
1	1.16	1.09	1.16	1.09	1.09
10	0.18	0.18	0.24	0.17	0.17
20	−0.51	−0.39	−0.40	−0.40	−0.35
30	−0.09	−0.10	0.07	0.13	0.12

	d (m), Y direction				
f (MHz)	−0.3	−0.15	0	0.15	0.3
1	1.51	1.33	1.16	1.33	1.45
10	0.39	0.29	0.24	0.29	0.33
20	−0.26	−0.28	−0.40	−0.28	−0.26
30	0.17	0.13	0.07	0.07	0.17

	d (m), Z direction				
f (MHz)	−0.3	−0.15	0	0.15	0.3
1	0.87	0.66	1.16	1.10	1.34
10	−0.17	−0.26	0.24	0.25	0.50
20	−0.75	−0.84	−0.40	−0.32	−0.18
30	−0.40	−0.36	0.07	0.08	0.21

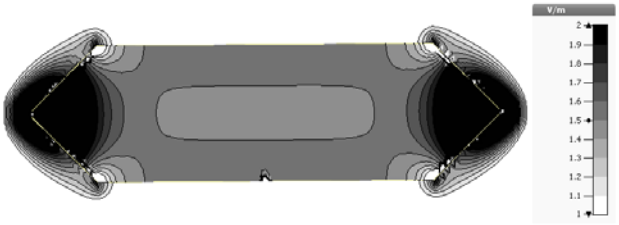

Figure 7. Simulated E-field magnitude at 1 MHz. XZ plane.

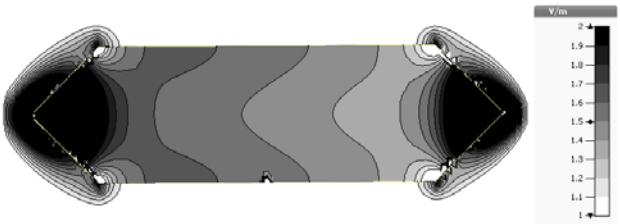

Figure 8. Simulated E-field magnitude at 30 MHz. XZ plane.

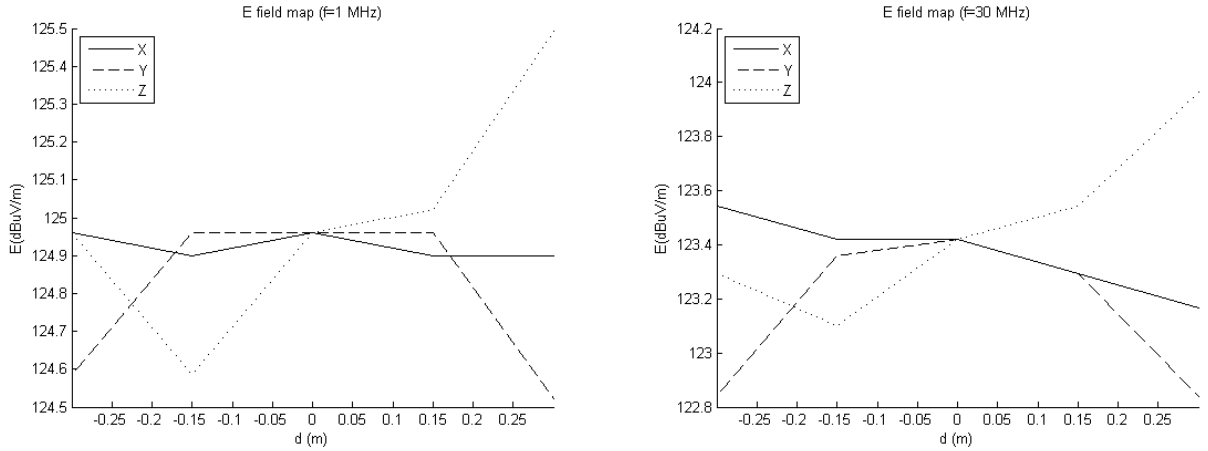

(a) Frequency 1 MHz (b) Frequency 30 MHz

Figure 9. Measurement of the E-field distribution along three directions.

probe. This measurement is made for an injected power of +10 dBm at all frequencies of interest. Then the loop is put in the middle of the cell and connected to the R&S ESH3 receiver (Figure 10). To avoid the antenna and receiver saturation, the injected power was reduced to −50 dBm. Since the magnitude of a measured E-field is proportional to the injected power, it is possible to apply Eq. (5) to obtain the gain.

After compensation of losses due to the cable feeding the cell, voltage deviation from the generator as well as balun losses, obtained results show a good agreement between measured and certified gains, with a delta of 1.15 dB at 1 MHz and 2.2 dB at 30 MHz (Figure 11).

Therefore, the measurement procedure can be done either by applying Eq. (5), which implies the measurement of the E-field amplitude and the voltage at the AUT terminals, or by a comparison with a reference antenna having a known gain. Hence, the AUT gain can be found simply by adding the reference antenna gain (expressed in dBi) to the difference of the voltage drops between the two antennas (expressed in dB).

3.2. Compared to Simulated Loop Antenna

Another comparison, this time concerning a simulated model, has been made. A loop of 30 cm diameter was considered in HFSS simulation software (Figure 12). The same geometry loop was built and measured by comparison with Lindgren 6502. A 1 : 1 balun ensures a symmetrical excitation of the antenna.

After compensation of losses due to the balun, the presented results show a good agreement with the simulated gain with a maximum deviation of 1.9 dB at 9 MHz (Figure 13).

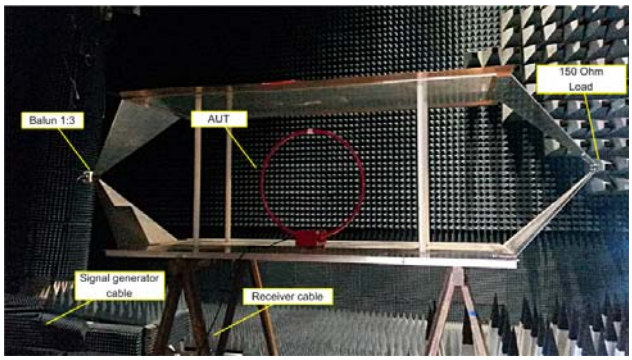

Figure 10. Measurement of the reference loop antenna Lindgren 6502.

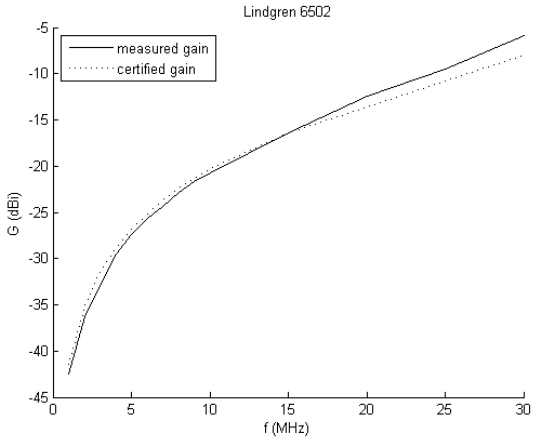

Figure 11. Gain measurement of the reference loop antenna Lindgren 6502.

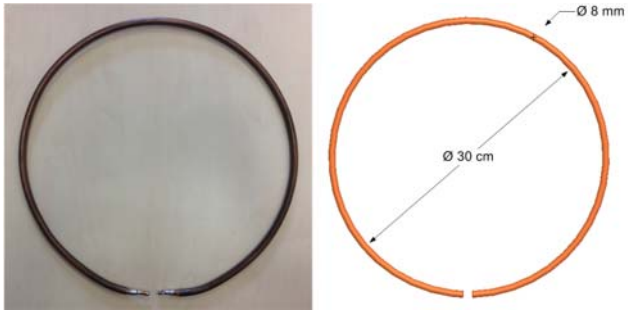

Figure 12. Loop antenna. Realized and simulated model.

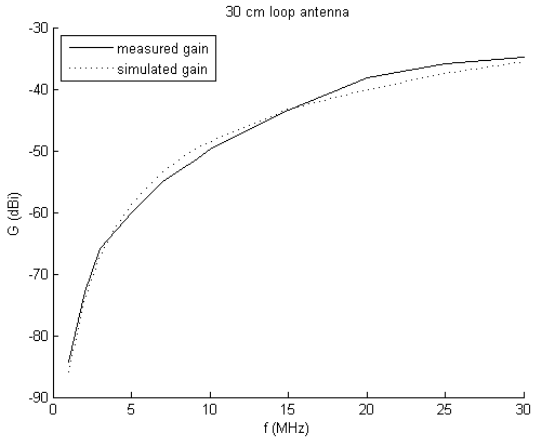

Figure 13. Gain measurement of the loop antenna.

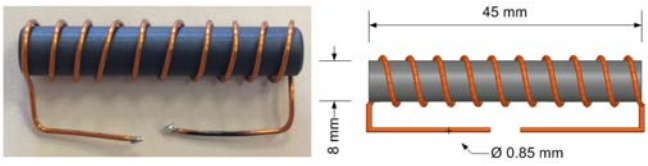

Figure 14. Solenoid antenna. Realized and simulated model.

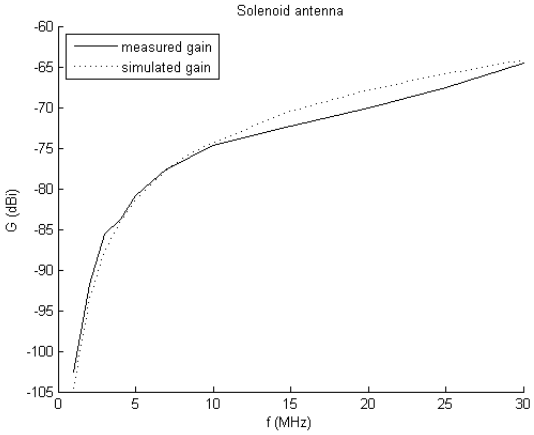

Figure 15. Gain measurement of ferrite solenoid.

3.3. Compared to Ultra Small Gain Ferrite Antenna

The proposed measurement method allows to measure very small antenna gains. To illustrate this, a 10 turn solenoid wrapped around a 61 material ferrite from Fair-Rite © was considered (Figure 14). As in the previous case, the antenna was connected to the balun whose insertion losses were compensated. The gain of less than −100 dBi was measured in this configuration and agrees with the simulation model from HFSS with a delta not exceeding 2.3 dB (Figure 15).

4. CONCLUSION

In this paper, a setup using a parallel plate cell has been investigated in order to measure the gain of miniaturized antennas in the HF band. The proposed installation is much simpler and less expensive than TEM/GTEM cells and allows much more space for the AUT. This method is also much less time-consuming and allows a well-defined environment compared to a free-space outdoor measurement. The validity of this technique has been demonstrated by a satisfying correlation not exceeding 2.3 dB, with a reference antenna as well as simulated models and even for very low gains about −100 dBi.

REFERENCES

1. Yaghjian, A. D., "An overview of near-field antenna measurements," *IEEE Transactions on Antennas and Propagation*, Vol. 34, No. 1, 30–45, 1986.
2. Stutzman, W. L. and G. A. Thiele, *Antenna Theory and Design*, Wiley, New Jersey, 2012.
3. Crawford, M. L., "Generation of standard EM fields using TEM transmission cells," *IEEE Transactions on Electromagnetic Compatibility*, Vol. 16, No. 4, 189–195, 1974.
4. Satav, S. M. and V. Agarwal, "Do-it-yourself fabrication of an open TEM cell for EMC pre-compliance," *IEEE EMC Society Newsletter*, No. 218, 66–71, 2008.
5. Iftode, C. and S. Miclaus, "Design and validation of a TEM cell used for radiofrequency dosimetric studies," *Progress In Electromagnetics Research*, Vol. 132, 369–388, 2012.
6. Nahman, N., M. Kanda, E. B. Larsen, and M. L. Crawford, "Methodology for standard electromagnetic field measurements," *IEEE Transactions on Instrumentation and Measurement*, Vol. 34, No. 4, 490–503, 1985.
7. Muterspaugh, M. W., "Measurement of indoor antennas using GTEM cell," *2003 IEEE International Conference on Consumer Electronics, 2003*, 126–127, 2003.
8. Zivkovic, Z. and A. Sarolic, "Gain and antenna factor measurements of broadband biconical dipole in the GTEM cell," *ELMAR, 2010 Proceedings*, 297–300, 2010.

9. Alaeldine, A., et al., "Efficiency of GTEM cell for measuring small antennas gain with respect to power losses calculation," *2011 IEEE International Symposium on Antennas and Propagation (APSURSI)*, 1898–1901, 2011.
10. Ivkovi, Z. and A. Aroli, "Gain and impedance measurement of microstrip patch antennas in GTEM cell," *2010 IEEE Conference Proceedings ICECom*, 1–4, 2010.
11. Icheln, C., P. Vainikainen, and P. Haapala, "Application of a GTEM cell to small antenna measurements," *IEEE Antennas and Propagation Society International Symposium, 1997*, Vol. 1, 546–549, 1997.
12. Hui, P., "Small antenna measurements using a GTEM cell," *IEEE Antennas and Propagation Society International Symposium, 2003*, Vol. 4, 715–718, 2003.
13. Roseberry, B. E. and R. B. Schulz, "A parallel-strip line for testing RF susceptibility," *IEEE Transactions on Electromagnetic Compatibility*, Vol. 7, No. 2, 142–150, 1965.
14. Morgan, D., *A Handbook for EMC Testing and Measurement*, IET, Stevenage, 1994.